

NUMERICAL OPTIMIZATION OF ENHANCED HYPERVELOCITY LAUNCHER

J. S. BAI^{*}, AND Y. WANG[†]

^{*} Institute of Fluid Physics, CAEP
P. O. Box 919-105 Mianyang, Sichuan, P. R. China, 621900
e-mail: bjsong@foxmail.com

[†] Institute of Fluid Physics, CAEP
P. O. Box 919-105 Mianyang, Sichuan, P. R. China, 621900
e-mail: mishiwufeng@126.com

Abstract. The Eulerian code Multi-Fluid Piecewise Parabolic Method (MFPPM) is employed to investigate the effect of dimensions of the impactor on the velocity and planarity of the flier plate. A convex impactor is carried out to further improve the planarity and velocity, while keeping the impact velocity constant. Results indicate that 12 percent increase in flier velocity of the central position and about 70 percent improvement in the planarity at the muzzle of the extensional barrel is present in the optimal model considering the limited launch capability of the two-stage light-gas gun. In addition, the convex impactor leads to a conspicuous increase of the flier velocity in central part but a slight increase of the velocity in other portions, which results in the variation of the planarity. However, the planarity of the flier plate at a given time or position can be improved by tuning the dimensions of the impactor, and the flier plate keeps relative flat in a short duration. Further studies will concern on the decrease of the velocity difference in order to perform the EOS studies.

Key Words: *Numerical Optimization, Enhanced Hypervelocity Launcher, MFPPM.*

1 INTRODUCTION

It is an important technique to launch the flyer plate to exceed 10 km/s in researching the high-pressure equation of state (EOS) of materials. Recently, Sandia has developed a HyperVelocity Launcher [1] (HVL for short), which is capable to launch the gram size flier plate to over 10km/s. There are two crucial conditions to launch the flier plates to hypervelocities, one is the very high pressure and acceleration, and the other is that the

pressure must be uniform, structured, and shockless to prevent the flier plate from either melting or fracturing [2,3]. These criterions are achieved by using a grade density material referred as ‘Pillow’ [4] or ‘Multi-ply’ [5,6] to impact the flier plate. Not only does the flyer plate remain satisfied flight attitude, but also has small temperature increment, small distortions and no fracture. It was reported that a 1 mm thick aluminum, magnesium and titanium alloy plates were accelerated to velocities over 10 km/s, and 0.5 mm thick aluminum and titanium alloy plates were launched to velocity of 12.2km/s by the HVL [2,3]. However, the hypervelocity of the chunk flier could be attained by the Enhanced HyperVelocity Launcher (EHVL), which is composed of a two stage light gas gun and a sacrificial extensional barrel [7-9]. This facility allows the launch of a 1 mm thick titanium alloy flier plate to a velocity of 14.4 km/s, and a 0.5mm thick titanium flier plate to a velocity of 15.8 km/s [10]. Velocity of 19 km/s in the titanium alloy flier was also realized [11].

By far a multitude of EOS studies has been carried out by HVL, but there is little information available in literature about the EOS studies performed on EHVL. A crucial problem is that the two-dimensional effects due to radial reshock waves (generated upon impact of the tungsten barrel) emanating from the edges of the plate may cause the edges to travel faster than the center of the flier plate initially [10]. These different loading histories cause the bending and large deformation of the flier plate, which pose a challenge to EOS studies. In this paper, we employed a Eulerian code MFPPM to further increase the chunk flier velocity based on the conventional setup carried out by the National Key Laboratory for Shock Wave and Detonation (LSD) Physics Research, and investigate the feasibility of the EOS studies performed on EHVL. Furthermore, the effects of structures and dimensions of the impactor on the planarity and velocity of the flier plate are also discussed.

2 EQUATIONS AND ALGORITHMS

2.1 Basic Equations

Based on the volume of fluid model [12], we combine the PPM method [13] with the interface tracking, and apply it to Euler hydrodynamic equations. The Euler governing equations can be written as

$$\left\{ \begin{array}{l} \frac{\partial \rho}{\partial t} + \frac{\partial \rho u_j}{\partial x_j} = 0 \\ \frac{\partial \rho u_i}{\partial t} + \frac{\partial \rho u_j u_i}{\partial x_j} + \frac{\partial p}{\partial x_i} = 0 \\ \frac{\partial \rho E}{\partial t} + \frac{\partial (\rho u_j E + p u_j)}{\partial x_j} = 0 \\ \frac{\partial Y^{(s)}}{\partial t} + u_j \frac{\partial Y^{(s)}}{\partial x_j} = 0 \quad s = 1, 2, \dots, N-1 \end{array} \right. \quad (1)$$

Here, i and j represent the three directions of x , y , z , respectively, and the add criteria are implied; ρ , u_k ($k=i, j$), p are density, velocity and pressure of materials; E is the total energy of a unit mass; N is the number of species of media; $Y^{(s)}$ is the volume fraction of sth species and satisfies $\sum Y^{(s)}=1$. The total energy of a unit mass is given as

$$E = e + (u_x^2 + u_y^2 + u_z^2)/2 \quad (2)$$

where e is the specific energy. A simplified Gruneisen EOS is used in this paper, and the form is as follow

$$p = (\gamma - 1)\rho e + c_0^2(\rho - \rho_0) \quad (3)$$

where γ is the constant of material, ρ_0 , c_0 is the density and sound speed under the normality respectively.

2.2 Multi-Fluid PPM Method

A two-step Lagrange/Remap algorithm is adopted to solve multi-fluid problems. The first step is the Lagrangian step in which the computation cells distort to follow the material motion. The one dimensional Lagrange equation for multi-fluid can be written as

$$\begin{cases} \frac{\partial \tau}{\partial t} - \frac{\partial(r^\alpha u)}{\partial m} = 0 \\ \frac{\partial u}{\partial t} + r^\alpha \frac{\partial p}{\partial m} = 0 \\ \frac{\partial E}{\partial r} + \frac{\partial(r^\alpha up)}{\partial m} = 0 \\ \frac{\partial Y^{(s)}}{\partial t} = 0 \end{cases} \quad (4)$$

where τ is the specific volume, α equals 0, 1, 2 corresponding to plane, axial symmetry and spherical symmetry problems, respectively. r is the spatial coordinate, and m is the mass coordinate defined as

$$m = \int_{r_0}^r \rho r^\alpha dr \quad (5)$$

The second step is the Remap step where the distorted cells are mapped back to the Eulerian meshes. In this step, the piecewise parabolic interpolation and integral method are the same as those in the Lagrange step. After the Remap step, we update the physical quantities in Euler mesh. This process can be extended to 2D and 3D easily according to the spatial operator-split algorithm. Moreover, in order to effectively capture interfaces of the materials, the two-step Lagrange/Remap algorithm applied to Eq. (1) can be divided into four steps: the piecewise parabolic interpolation of physical quantities, the approximately solution of the Riemann problems, the evolution of the Lagrange equations and the mapping of the physical quantities back onto the Euler meshes.

The verification and validation of MFPPM [14,15] are carried out with HVL and EHVL reported by Sandia National Laboratories. Numerical results of flier velocities excellently agree with the experimental and numerical results of Sandia, and the maximum relative error is less than 1.1%. MFPPM has been used to investigate the hypervelocity launch [15-17] and instability problems [18,19].

3 RESULTS AND DISCUSSION

Present study aims at improving the velocity and planarity the flier plate in the initial model. In order to describe the planarity in digitization, a parameter δ is introduced and denotes the distance between the highest and lowest positions of deformed free surface, while the two peaked edges in the case illustrated in Figure 1b is neglected. Moreover, D and H represent the diameter and thickness of the tungsten layer, respectively, and R is the radial position on the free surface of the flier plate. In order to discriminably describe the large number of calculations in present study, we commonly use Model 25-1.2 (initial model) to represents the calculation with 25 mm in diameter and 1.2 mm in thickness of the tungsten layer.

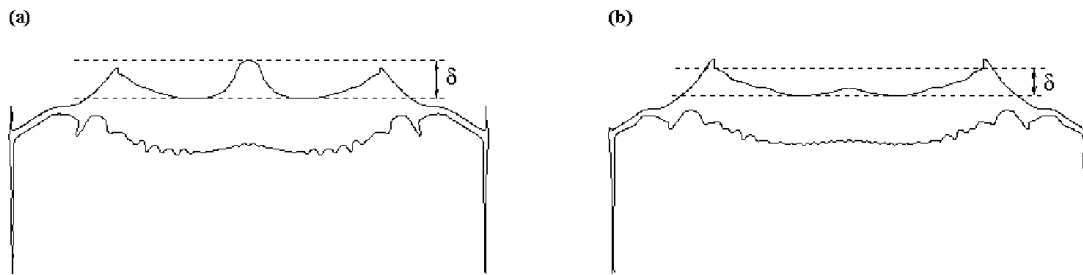


Figure 1: Definitions of planarity parameters δ .

Table 1: Parameters of multi-ply grade-density impactor, flier plate and TPX buffer in initial model.

Multi-ply Grade-Density Impactor Assembly PMMA/MB2/Al/TC4/Cu/93W Thickness(mm)	Grade-Density Impactor Diameter (mm)	Impact Velocity (km/s)	Flier Plate Material	Flier Plate Thickness/Diameter (mm)	TPX Buffer Diameter (mm)	Barrel Material/Length (mm)
0.9/0.35/0.3/0.28/0.32/1.2	25	6.8	Ta	0.5/10	28	tungsten/10

The initial model is defined as follows: A grade-density impactor housed by a lexan projectile is fabricated by bonding a series of thin plates varied in shock impedance. The lowest impedance material is placed at the impact side, with impedance increasing as the depth in the impactor increases, as shown in Figure 2. The series of layers consists of poly methyl meth acrylate (PMMA), magnesium-aluminum alloy, aluminum, titanium alloy,

copper, and tungsten, the thickness of each layers as well as other parameters are listed in Table 1

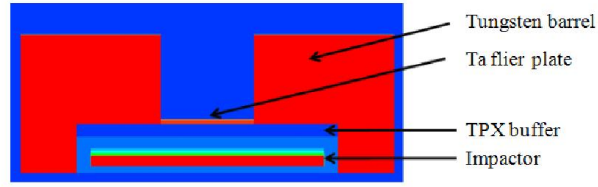


Figure 2: Schematic of the initial model

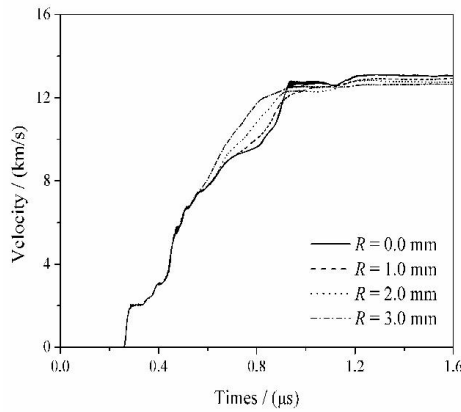


Figure 3: Velocity histories of the flier plate at different radial positions in the initial model.

The velocity histories on the free surface of the flier plate are depicted in Figure 3. The velocities of four different positions are identical during the initial loading. Then the two-dimensional effects due to radial reshock waves emanating from the edges of the plate causes the two edges go faster than the central portion of the plate. As a result, the velocity differences appear at about $0.57\mu\text{s}$ and increase with time before the impactor impacts the extensional barrel. This results in a concave bending of the flier plate, as shown in Figure 4. After that, the velocities increase rapidly due to the further acceleration within the stepped barrel, and finally keep relative steady. The steady velocities of four positions are 13.08 km/s, 12.89 km/s, 12.78 km/s and 12.66 km/s (from inner to outer), and the planarity parameter δ is 0.488 at $1.4\mu\text{s}$. Compared with HVL, the greater velocity differences and worse planarity are present at the expense of the velocity enhancement of EHVL. Loading by EHVL, the flier experiences a deformation history from concave bending to convex bending due to the changes of the velocity difference. Therefore, there should be a short duration during which the flier keeps relatively flat, which is crucial for EOS studies. However, the determination of this duration is facile in numerical studies but difficult in experiments.

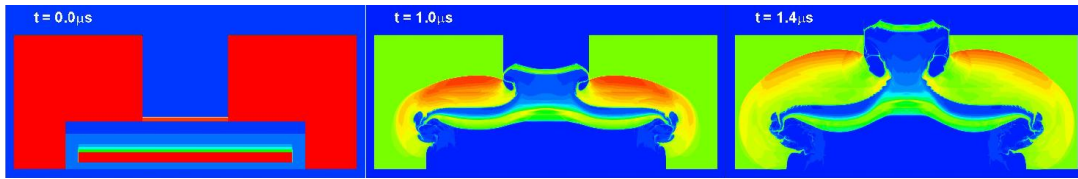


Figure 4: The density contours of the filer plate in the initial model at different times.

The concave impactors are conducted via varying the dimensions of the tungsten layer and keeping the other layers invariable, as shown in Figure 5. A series of simulations is carried out with various diameters and thicknesses of the tungsten layer. The impact velocity is set as 6.8 km/s. It should be pointed out that not all the impact velocities in simulations will be obtained in the experiment due to the limited launch capability of the two-stage light-gas gun. Figure 6 shows the mass differences of the impactor in all models, the horizontal dash line represents the zero contours. Models over this line will add additional mass to the projectile, which lowers the impact velocity to less than 6.8 km/s. However, this does not inhibit us from exploring the effects of chunk fliers on the planarity, velocity and velocity difference, while care must be taken in the experiments.

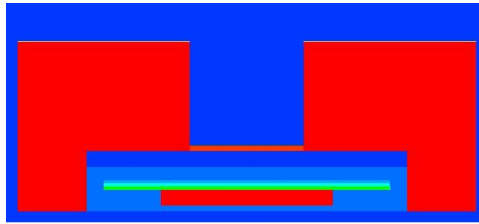


Figure 5: The density contours of the filer plate in the initial model at different times.

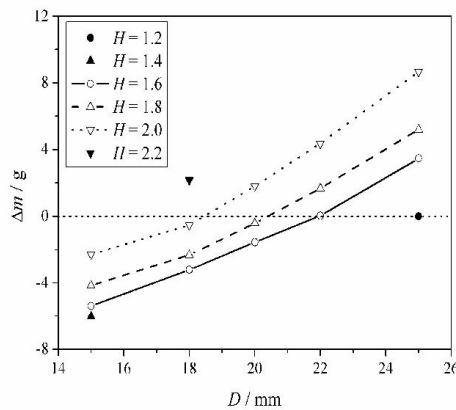


Figure 6: The mass difference of the impactor as a function of the diameter and thickness of the tungsten. The horizontal dashed line represents the zero contours of the mass difference.

The effects of the diameter and thickness on the flier velocity and planarity at $1.4 \mu\text{s}$ is present in Figure 7. Assume that the impact velocity of 6.8 km/s is available in every simulation, the maximum velocity of 15.3 km/s is achievable, and the corresponding amplification ratio is 2.25. In all calculations, only the velocity of Model 15-1.4 is lower than that of initial model, but a significant mass decrease is present, with which a higher impact velocity can be attained. Moreover, all planarity parameters δ are smaller than that of initial model, which indicates an improvement of the planarity. As the diameter increases, the flier velocity increases and planarity decreases more and more slowly while keeping the thickness constant. This tendency is similar as that when we increase the thickness and keep the diameter constant, and is partly related to the mass variation of the impactor. As the mass of the impactor increases, the forward momentum and kinetic energy transferred from the impactor to the flier plate are enlarged, which leads to the increase of the flier velocity. Another possible reason for the velocity enhancement is that the increase of the mass ratio of the tungsten in the impactor contributes to the flier velocity. This can be demonstrated by a comparison between Model 22-1.6 and the initial model. These two models have the same mass of the impactor, but differ in the mass ratio of tungsten. Model 22-1.6, with a higher mass ration of tungsten, provides a higher velocity. As a result, the high velocity, together with the change of the velocity difference discussed in the initial model, improve the planarity of the flier plate at the muzzle of the extensional barrel.

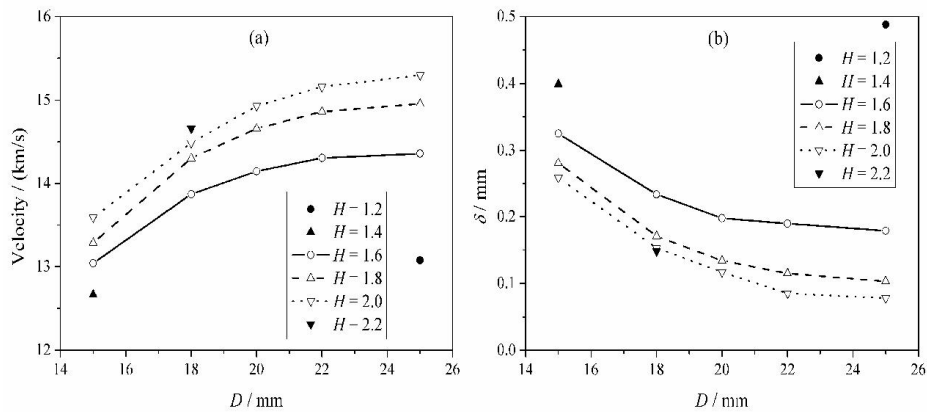


Figure 7: The velocity and planarity of the flier plate as a function of the diameter and thickness of the tungsten at $1.4 \mu\text{s}$. The black solid dot denotes the result of initial Model.

Considering the launch capability of the two-stage light-gas gun and the slighter variations of the velocity and planarity, model 20-1.8 is chosen as the optimal one. As compared to the initial model at $1.4 \mu\text{s}$, 3% decrease in mass of the impactor and 72.5% decrease in planarity parameter δ , as well as 12% increase in flier velocity of the center position are realized in the optimal model.

4 CONCLUSIONS

The Eulerian code MFPPM is employed to numerically investigate the ways of improving the flier velocity and planarity via employing a convex impactor. The effects of the dimensions of the impactor is also carried out. The convex impactor contributes to the improvement of the flier velocity and the planarity at the muzzle of the extensional barrel due to the increase of the mass of the impactor and the mass ratio of the tungsten. The increase of the flier velocity and planarity becomes more and more slowly as the thickness or diameter of the tungsten layer increase while keeping the other constant. Model 20-1.8 is chosen as the optimal model on account of the limited launch capability of the two light gas gun and the laggardly variations of the velocity and planarity with a large diameter or thickness. 12.5% increase in the velocity and 75% decrease in the planarity can be realized in the optimal model.

It should be noted that the material strength does not play a large role in the hypervelocity launch. Thus, present study does not take it into consideration. In addition, recent studies shows that the velocity difference across the surface of the flier plate increases with the above optimization. Further studies will focus on the decrease of the velocity difference.

The work was sponsored by the National Science Foundation of China Grant No. 11372294.

REFERENCES

- [1] Trucano, T. G. and Chhabildas, L. C. Sandia's New HyperVelocity Launcher-HVL. Sandia National Report, SAND91-0657(1991).
- [2] Chhabildas, L. C. Hypervelocity launch capabilities to over 10 km/s. Sandia National Report, SAND91-1374C(1991).
- [3] Chhabildas, L. C., Dunn, J. E. and Reinhart, W. D., et al. An impact technique to accelerate flier plates to velocities over 12 km/s. *Int. J. Impact Engng*(1993) **14**:121-132.
- [4] Barker, L. M. High-pressure quasi-isentropic impact experiments. In: *Shock Waves in Condensed Matter 1983*, (Asay J. R., Graham R. A. and Straub G. K. eds.), Elsevier Science Publishers, B. V.(1984):217-224.
- [5] Chhabildas, L. C. and Barker, L. M. Dynamic quasi-isentropic compression of tungsten. In: *Shock Waves in Condensed Matter 1987*, (Schmidt S. C. and Holmes N. C. eds.), Elsevier Science Publishers, B. V.(1988):111-114.
- [6] Chhabildas, L. C., Asay, J. R. and Barker, L. M. Shear strength of Tungsten under shock- and quasi-isentropic loading to 250 GPa. Sandia National Report, SAND88-0306(1988).
- [7] Trucano, T. G. and Chhabildas, L. C. Calculations supporting HyperVelocity Launcher development. Sandia National Report, SAND93-0402C(1993).

- [8] Chhabildas, L. C., Trucano, T. G. and Reinhart, W. D., et al. "Chunk" Projectile Launch Using The Sandia Hypervelocity Launcher Facility. Sandia National Report, SAND 94-1273(1994).
- [9] Trucano, T. G. and Chhabildas, L. C. Computational design of hypervelocity launchers. *Int. J. Impact Engng*(1995) **17**:849-860.
- [10] Chhabildas, L. C., Kmetyk, L. N. and Reinhart W. D., et al. Enhanced hypervelocity launcher capabilities to 16km/s. *Int. J. Impact Engng*(1995) **17**:183-194.
- [11] Thornhill, T. F., Chhabildas, L. C. and Reinhart, W. D., et al. Particle launch to 19 km per s for micro-meteoroid simulation using enhanced three-stage light gas gun hypervelocity launcher techniques. *Int. J. Impact Engng*(2006) **33**:799-811.
- [12] Hankin, R. K. S. The Euler equations for multiphase compressible flow in conservation form: simulation of shock - bubble interactions. *Journal of Computational Physics*(2001) **172**(2):808-826.
- [13] Corlella, P. and Woodward, P. R. The piecewise parabolic method (PPM) for gas-dynamical simulations. *Journal of Computational Physics*(1984) **54**:174-201.
- [14] Bai, J. S., Tan, M. and Hua, J. S., et al. An improved of experimental hypervelocity launcher and simulation. *Chinese Journal of High Pressure Physics*(2007) **21**(3):253-258.
- [15] Bai, J. S., Hua, J. S. and Tan, M., et al. Experimental research and numerical analysis for hypervelocity launch. *Chinese Journal of Applied Mechanics*(2008) **25**(2):177-180.
- [16] Bai, J. S., Tan, H. and Li, P., et al. Numerical simulation method for 2-d hypervelocity launcher under the graded density impactor drives. *Chinese Journal of Computational Physics*(2004) **21**(4):305-310.
- [17] Bai, J. S., Shen, Q. and Tan, M., et al. A numerical analysis of the influence of buffer material on tantalum flier plate velocity in the hypervelocity launcher. *Chinese Journal of High Pressure Physics*(2008) **22**(1):19-24.
- [18] Bai, J. S., Li, P. and Chen, S. H. et al. Numerical Simulation of the Instability of the Jelly Surfaces under the Imploding Drives. *Chinese Journal of High Pressure Physics*(2004) **18**(4):295-301.
- [19] Bai, J. S., Li, P. and Tan, D. W., et al. Numerical study of the interface instability experiment. *Chinese Journal of Theoretical and Applied Mechanics*(2007) **39**(6):741-748.